Carbohydrate Polymers 86 (2011) 1784–1789

Contents lists available at ScienceDirect

Carbohydrate Polymers

journal homepage: www.elsevier.com/locate/carbpol

Structure and properties of starch/PVA/nano-SiO_2 hybrid films

Kunhua Yao[a,b], Jie Cai[a,b], Miao Liu[a,b], Yan Yu[c], Hanguo Xiong[a,b,*], Shanwen Tang[a,b], Shiyong Ding[a,b]

[a] College of Food Science and Technology, Huazhong Agricultural University, Wuhan 430070, China
[b] Research Institute of Comprehensive Utilization of Biomaterials, Huazhong Agricultural University, Wuhan 430070, China
[c] International Central for Bamboo and Rattan, Beijing 100102, China

ARTICLE INFO

Article history:
Received 13 June 2011
Received in revised form 3 July 2011
Accepted 9 July 2011
Available online 19 July 2011

Keywords:
Biodegradable film
Nano-silicon dioxide
Corn starch
Structure
Properties

ABSTRACT

Starch/polyvinyl alcohol (PVA)/nano-silicon dioxide (nano-SiO_2) biodegradable hybrid films were prepared via the sol–gel method. Fourier transform infrared spectroscopy, scanning electron microscopy, and X-ray photoelectron spectroscopy were used to evaluate the structure of the films. The aging and biodegradable properties of the films were studied as well. A gel network was formed in the films; this network is responsible in improving the performance of the starch/PVA/nano-SiO_2 hybrid films. The crystal structure of the films was increased owing to the addition of nano-SiO_2. The addition of nano-SiO_2 also delays aging of the films. However, the enzymatic degradation test shows that the addition of nano-SiO_2 has no significant influence on the biodegradability of the films.

1. Introduction

The past few years have seen a renewed interest in films made from renewable and natural polymers such as starch (Mali, Grossmann, Garcia, Martino, & Zaritzky, 2002; Mathew & Abraham, 2008). Starch is considered as a suitable source material because of its inherent biodegradability, accessibility, and relatively low cost (Bandyopadhyay, Bhowmick, & Sarkar, 2005; Bangyekan, Aht-Ong, & Srikulkit, 2006; Ishigaki, Kawagoshi, Ike, & Fujita, 1999; Jayasekara, Harding, Bowater, Christie, & Lonergan, 2004). However, the use of starch in the preparation of starch-based biomaterials such as packaging films and agricultural plastic films is limited by its multi-hydroxyl and regular crystal structure (Park, Chough, Yun, & Yoon, 2005; Zhang, Xu, Xia, Zhang, & Yu, 2006).

Starch/polyviny lalcohol (PVA) blend plastics are one of the most popular biodegradable plastics widely used in packaging and agricultural applications (Follain, Joly, Dole, & Bliard, 2005; Xiao & Yang, 2006; Zhai, Yoshii, & Kume, 2003; Zhai, Yoshii, Kume, & Hashim, 2002). Polyvinyl alcohol is a biodegradable synthetic material which promotes good film formation, strong conglutination, and high thermal stability. In recent years, the application of PVA in the material industry has increased (Funke, Bergthaller, & Lindhauer, 1998). However, the mechanical properties and water resistance of the native starch/PVA film are still inferior to those of polymers made from petroleum.

In this experiment, the starch/PVA blended films are modified by nano-SiO_2. Studies indicate that nano-materials improve the performance of polymer materials such as plastic and rubber (Chaichana, Jongsomjit, & Praserthdam, 2007; Xiong, Tang, Tang, & Zou, 2008; Yu, Dean, & Li, 2006); however, relevant studies on starch polymers modified by nano-SiO_2 have not yet been reported (Yang et al., 2006; Zou et al., 2007).

Nano-SiO_2 can be used to modify starch/PVA blended films owing to its multi-hydroxyl structure and high surface activity. The structure of the starch/PVA/nano-SiO_2 hybrid film was characterized by Fourier transform infrared (FT-IR) spectroscopy, X-ray photoelectron spectroscopy (XPS), X-ray diffraction (XRD), and scanning electron microscopy (SEM); the aging and biodegradable properties were obtained in the laboratory. By studying the effect of nano-SiO_2 on the structure and properties of the starch film, the mechanism for improving the properties of a starch-based biodegradable films using nano-SiO_2 was determined.

2. Materials and methods

2.1. Materials

Nano silicon dioxide (nano-SiO_2), with a particle size of 60 nm, was provided by the Nanometer Engineering Center of the People's Republic of China. Corn starch (ST) was provided by Huanglong

* Corresponding author at: College of Food Science and Technology, Huazhong Agricultural University, Wuhan, Hubei 430070, China. Tel.: +86 27 87288377; fax: +86 27 87286608.
E-mail address: xionghanguo@163.com (H. Xiong).

0144-8617/$ – see front matter © 2011 Elsevier Ltd. All rights reserved.
doi:10.1016/j.carbpol.2011.07.008

Table 1
Experimental ingredients and nomenclatures of films.

Samples	ST (g)	PVA (g)	Glycerine (g)	SiO_2 (g)	Water (ml)
SP	6	4	3	0	125
NSP1	6	4	3	0.1	125
NSP2	6	4	3	0.2	125
NSP3	6	4	3	0.3	125
NSP4	6	4	3	0.4	125
NSP5	6	4	3	0.5	125
NSP6	6	4	3	0.6	125
NSP7	6	4	3	0.7	125
NSP8	6	4	3	0.8	125

Food Ltd. of Gongzhuling City (moisture content 11.7%, protein 0.23%, fat 0.075%, and ash content 0.08%), while polyvinyl alcohol (PVA) was produced and provided by Chongqing Inorganic Chemical Reagent Factory (DP 1799 ± 50, NaOH $\leq 0.2\%$, acetic acid remnant $\leq 0.13\%$, volatilization content $\leq 9.0\%$, and transmissivity $\geq 90\%$). Tetraethyl orthosilicate (TEOS) and the ethanol used, which were of analytical grade, were purchased from Aldrich. The water used was distilled and deionized water. Then glycerine and other reagents, which were all of analytical grade, were used as received.

2.2. Preparation of the films

Aqueous 8 wt.% ST/PVA solutions were prepared by dissolving 6 g of ST and 4 g PVA in 125 ml deinoized water, and then it was stirred with certain speed (=500 rpm) in a constant temperature water bath at 90 °C for 30 min. Then 3 g of glycerine was mixed, and the mixture was stirred for 90 min before casting into a plexiglass plate placed on a leveled flat surface. After the blends were allowed to dry at 40 °C in an oven for 12 h, the fully dried membranes were peeled away from the glass plate, then they were heated in a thermosetting oven at 95 °C for 1 h to induce cross-linking reaction.

For comparison purposes, The ST/PVA/nano-SiO_2 composites were prepared by the addition of a TEOS mixture to the 8 wt.% ST/PVA solutions. The TEOS mixture was prepared by mixing H_2O, HCl, and TEOS in a molar ratio of 4:0.1:1, which was stirred with certain speed at 30 °C for 30 min. The TEOS was added at a different weight to the polymer weight. Then the ST/PVA/TEOS solutions were mixed together along with 3 g of glycerine for each composition, and the mixture was stirred at 90 °C for 2 h. The solutions were then poured onto a plexiglass plate. The cast solutions were allowed to dry at 50 °C for 12 h. After which, the fully dried membranes were peeled away from the glass plate, and then were heated in a thermosetting oven at 95 °C for 1 h to induce the crosslinking reaction. The experimental ingredients used to prepare the films and the nomenclatures used for each sample are shown in Table 1.

2.3. IR analysis of the films

The powdered samples were blended with potassium bromide (1:200) and laminated, and the IR spectra were recorded with a Nicolet (USA) Nexus 470 FT-IR spectrometer. The wave range, from 4000 to 400 cm^{-1}, was scanned 32 times for spectrum integration. The scanning resolution was 4 cm^{-1}. The relative crystal index was calculated using Eq. (1).

$$R = \frac{A_c}{A_t} = \frac{A_c}{A_c + A_a} = \frac{A_{993} + A_{1055}}{A_{993} + A_{1055} + A_{1022}} \quad (1)$$

where A_c is the crystalline area, A_a is the amorphous area and A_t is the total area. A_{993}, A_{1055} and A_{1022} are the absorption peak areas at 993 cm^{-1}, 1055 cm^{-1} and 1022 cm^{-1} respectively.

2.4. SEM analysis of the films

The cross section of the blend films was observed using a JSM-6390/LV scanning electron microscope (SEM) with the accelerating voltage of 30 kV. All specimens were coated with gold and then observed.

2.5. XPS analysis of the films

X-ray photoelectron spectroscopy (XPS) was conducted using a Perkin-Elmer PHI 5600 ESCA system. The surface of the NSP5 was scanned to analyse elements.

2.6. Aging properties test

Aging experiment of starch/PVA/nano-SiO_2 hybrid films: the films were placed in homemade UV aging box (quartz UV lamp 60 W), with the rough facing up, the sample surface 30 cm away from the UV lamp and distance between samples not less than 10 mm. At certain time interval, the samples were taken out for testing, and the experiment lasted 60 days.

Aging characteristics researched by infrared spectroscopy: at certain time interval, the samples were taken out, and the IR spectra of which were determined.

2.7. Biodegradable properties test

Enzymatic degradation test: after the 8 cm × 8 cm sheet films were dried at 90 °C to a constant weight, 250 ml of distilled water was added. And then, it was stirred with low speed in a constant temperature water bath at 60 °C, adjusting PH value of 6.9 and adding 1% α-amylase (quality, dry) into it. After enzymatic degradation for a certain time, the residue was washed with water, dried at 90 °C to a constant weight and weighed. The weight loss rate was calculated as follow:

$$\text{Weight loss rate}\,(\%) = \frac{W_0 - W_1}{W_0} \times 100\% \quad (2)$$

where W_0 is the quality of the sample before enzymatic degradation (g), W_1 is the quality of the sample after enzymatic degradation (g).

3. Results and discussion

3.1. IR analysis

The IR spectrum of SP and NSP films (a) and the peak position for the O–H stretching of the films (b) are shown in Fig. 1 Fig. 1. The absorption peak of –OH of NSP1 shifted to a wave number lower than that of SP; this is caused by the hydrogen bonds formed when the free –OH of nano-SiO_2 combines with that of ST/PVA. From NSP2 to NSP5, the absorption peak of –OH continuously shifted to a higher wave number, indicating a decrease in hydrogen bonds. A possible explanation for this is that upon saturation of the reaction between the free –OH of nano-SiO_2 with that of ST/PVA, the –OH on the surface of nano-SiO_2 competed for the hydrogen bond –OH formed within the ST and the PVA molecules as well as between the ST and PVA molecules. Consequently, new hydrogen bonds were formed, resulting in the formation of intermolecular hydrogen bonds between nano-SiO_2 and ST or between nano-SiO_2 and PVA, thus disrupting the orientational structure formed by intermolecular hydrogen bond association. The absorption peak of the –OH of the films therefore shifted to a higher wave number.

For a more detailed analysis of the IR spectroscopy of the casting films, the Peakfit software was selected for the deconvolution of the IR absorption spectra of SP and NSP at the

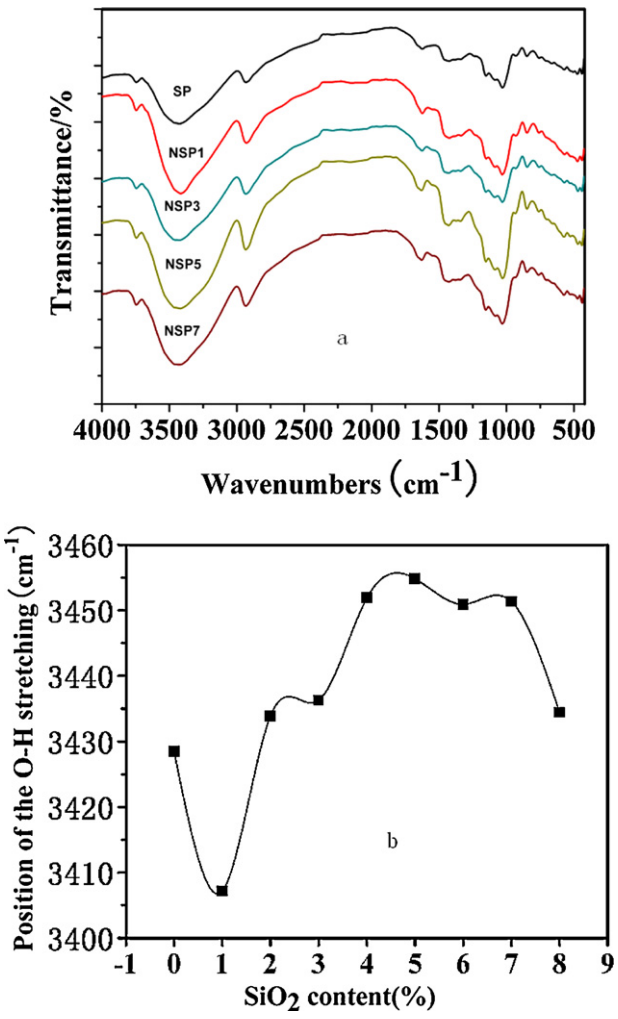

Fig. 1. The IR spectrum of SP and NSP films (a) and the peak position for the O–H stretching of the films (b).

range of 900–1200 cm^{-1} after taking the baseline. In the fingerprint area of the IR spectra of the films, the absorption peak at 1055 cm^{-1} was attributed to the crystal structure in the aggregation state of starch and PVA. The absorption peak at 993 cm^{-1} was attributed to the hydrogen bond formed between the –OH of starch and that of the PVA macromolecules; this is closely related to the short-range ordered structure of starch and PVA. The shape of the absorption peak in this position is relevant to intramolecular water content. The absorption peak at 1022 cm^{-1} was attributed to the random coil structure of starch and PVA macromolecules. The proportion between the ordered and the random coil structures in the starch molecule is reflected by the calculated ratio of the absorption peak areas: $R_1 = A_{993/1022}$ and

Table 2
IR deconvolution area of SP and NSP films.

Samples	993 cm^{-1}	1022 cm^{-1}	1055 cm^{-1}
SP	0.94297	1.48861	0.82222
NSP1	1.20986	1.88741	0.56079
NSP2	1.34012	2.00241	0.73414
NSP3	1.96058	2.64608	0.97848
NSP4	2.11814	1.96306	0.75728
NSP5	3.72612	3.18285	0.97579
NSP6	7.69823	7.45802	1.58303
NSP7	2.3576	2.71657	0.33887
NSP8	3.649	5.21089	0.57489

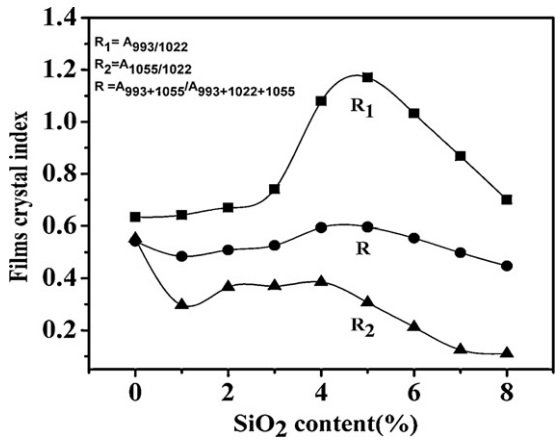

Fig. 2. Films crystal index on different SiO_2 contents.

$R_2 = A_{1055/1022}$; the relative crystal index was calculated using Eq. (1).

The IR deconvolution results of the SP and NSP films are shown in Fig. 2 and Table 2. After deconvolution, there was an apparent increasing trend in IR absorption peaks at 993, 1022, and 1055 cm^{-1} along with the increase of nano-SiO_2 content. The calculation of the change rule of R_1, R_2, and R with nano-SiO_2, revealed that R_1 increased along with the increase in nano-SiO_2 content, reaching a maximum point at about NSP5 ($R_1 = 1.17$). When the nano-SiO_2 content exceeded 5%, R_1 decreased as nano-SiO_2 content increased; however, R_1 is still much higher than that of SP films. The change of R_1 value also reveals that a large number of hydrogen bonds were formed in the films upon the addition of nano-SiO_2. This result is consistent with the peak position for the O–H stretching of films (b) reflected in Fig. 1 and thus illustrates that the addition of nano-SiO_2 promotes the orderly arrangement of the short-range structure of starch and PVA molecular chains. The R_2 values of the NSP films are smaller than those of the SP films, indicating that the addition of nano-SiO_2 hindered the orderly arrangement of the long-range structure of starch and PVA molecular chains. Fig. 2 also shows that the addition of nano-SiO_2 has no significant influence on the relative crystal index.

3.2. SEM analysis

Fig. 3 shows the SEM micrograph of the cross section of the films. The cross section of SP is lamellar, whereas a clear microporous structure appears on the cross sections of the NSP3–NSP7 films, indicating that the gel network structure was formed by combining nano-SiO_2 with starch/PVA and the addition of SiO_2 sol.

The gel network structure was formed in the starch/PVA/nano-SiO_2 hybrid film because there was plenty of –OH on the nano-SiO_2 surface. Once nano-SiO_2 permeated into the molecular chains of ST and PVA, the gel network structure forms through the hydrogen bonds produced by combining the –OH of nano-SiO_2 with that of starch/PVA.

3.3. XPS analysis

Fig. 4 shows the elemental analysis of the NSP5 film surface. The main elements of the NSP5 surface were C, O, and Si. The experimentally determined value (1.23%) for the surface quality content of Si was lower than the theoretical value (1.73%), illustrating that nano-SiO_2 was involved in the crystallization with ST/PVA and was thus partly covered because it served as the crystallization nucleating agent.

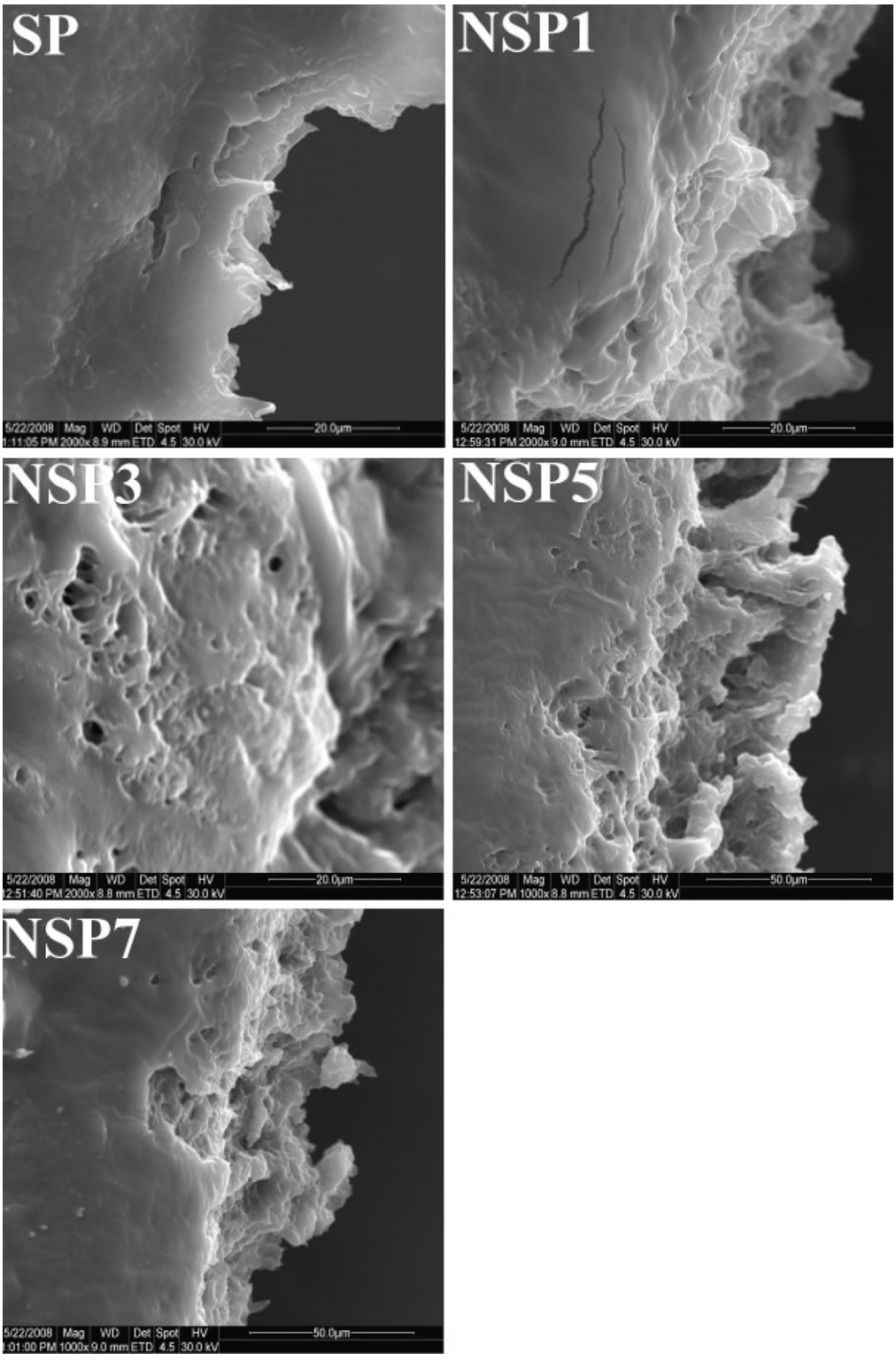

Fig. 3. SEM micrograph of the cross section of the films.

3.4. Aging properties by infrared spectrum analysis

The IR spectrum of SP and NSP5 on different ultraviolet aging times is shown in Fig. 5. It can be seen from the 4000 cm^{-1} to 500 cm^{-1} IR spectrum of the films that the IR spectrum changed largely near 2100 cm^{-1} and 1600 cm^{-1} with an increase in aging time. The new absorption peaks of C=C and C=O appeared at 2150 cm^{-1}, 2048 cm^{-1}, 1714 cm^{-1}, 1590 cm^{-1}, and 1648 cm^{-1} with the increase in aging time. The absorption peaks of NSP5 were weaker than those of SP, indicating that the degree of aging of NSP5 was lower than that of SP and that nano-SiO_2 delayed the aging of the films.

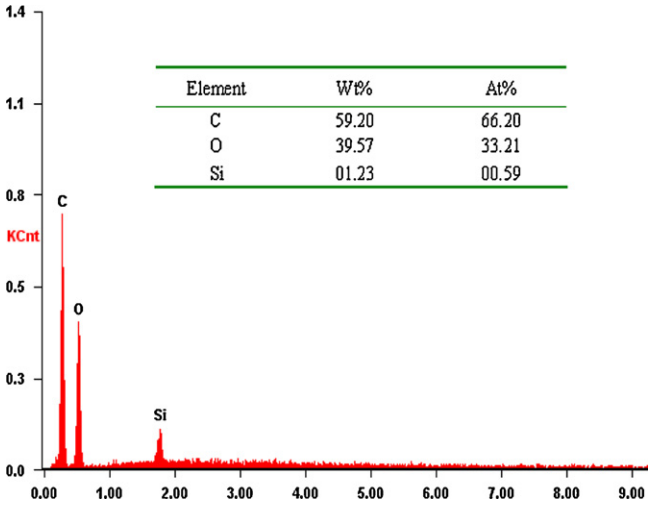

Fig. 4. Elemental analysis of the NSP5 film surface.

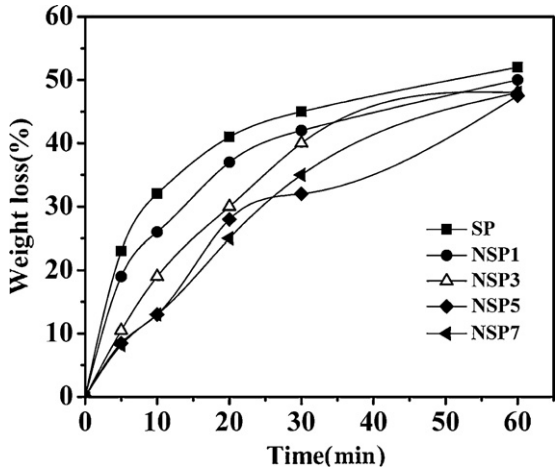

Fig. 6. Influences of SiO_2 on films weight loss rate by enzymatic degradation method.

3.5. Biodegradable properties

The influence of nano-SiO_2 on film weight loss rate via enzymatic degradation is shown in Fig. 6. The weight loss of SP was higher than that of NSP at the early stage of enzymatic degradation; SP and NSP had similar weight loss behavior at 60 min enzymatic degradation time. This might indicate that nano-SiO_2 had no significant influence on the biodegradability of the films. Through the enzymatic degradation method, nano-SiO_2 increased miscibility and compatibility; a dense structure was formed between ST and PVA, which in turn reduced the infiltration velocity of amylase, causing the weight loss in NSP to be lower than in SP in the early stage. However, with the increase in degradation time, the compactness of NSP was destroyed. The final

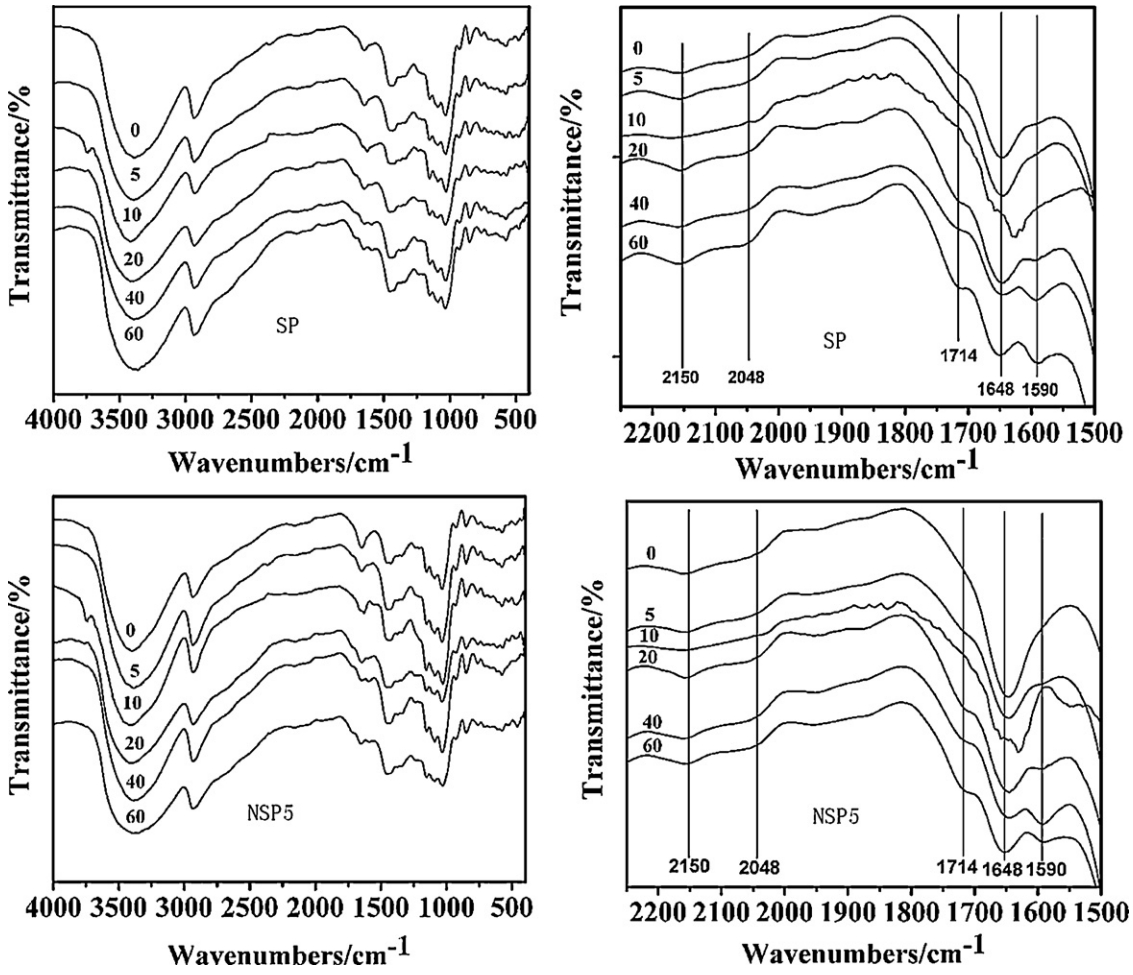

Fig. 5. IR spectrum of SP film and NSP5 film on different ultraviolet aging times.

biodegradability is related only to the starch content of the films. Therefore, both films exhibited the same weight loss at the later stage.

4. Conclusions

The properties of a starch/PVA/nano-SiO_2 hybrid film were improved through the addition of nano-SiO_2. IR analysis reveals that intermolecular hydrogen bonds were formed between nano-SiO_2 and ST or between nano-SiO_2 and PVA. The cross section morphology of NSP films indicates the formation of a gel network structure. XPS analysis shows that nano-SiO_2 may be involved in crystallization with ST/PVA.

The aging test indicates that the addition of nano-SiO_2 delays the aging of the films, but aging occurred nonetheless. The experiment also showed that the addition of nano-SiO_2 has no significant influence on the biodegradability of the films, the final biodegradability is related only to the starch content. The enzymatic degradation test reflects that the structure of the NSP membrane is denser than that of the SP membrane.

Acknowledgement

We acknowledge the financial assistance support for this work from the Special Fund for Scientific Research of the Forest in the Public Interest (No.201204808) and the National Natural Science Foundation of China (No.20976066).

References

Bandyopadhyay, A., Bhowmick, A. K., & Sarkar, M. D. (2005). Polyamide-6, 6/in situ silica hybrid nanocomposites by sol–gel technique: Synthesis, characterization and properties. *Polymer*, *46*(10), 3343–3354.

Bangyekan, C., Aht-Ong, D., & Srikulkit, K. (2006). Preparation and properties evaluation of chitosan-coated cassava starch films. *Carbohydrate Polymers*, *63*, 61–71.

Chaichana, E., Jongsomjit, B., & Praserthdam, P. (2007). Effect of nano-SiO_2 particle size on the formation of LLDPE/SiO_2 nanocomposite synthesized via the in situ polymerization with metallocene catalyst. *Chemical Engineering Science*, *62*, 899–905.

Follain, N., Joly, C., Dole, P., & Bliard, C. (2005). Properties of starch based blends. Part 2. Influence of polyvinyl alcohol addition and photo crosslinking on starch based materials mechanical properties. *Carbohydrate Polymers*, *60*, 185–192.

Funke, U., Bergthaller, W., & Lindhauer, M. G. (1998). Processing and characterization of biodegradable products based on starch. *Polymer Degradation and Stability*, *59*, 293–296.

Ishigaki, T., Kawagoshi, Y., Ike, M., & Fujita, M. (1999). Biodegradation of a polyvinyl alcohol–starch blend plastic film. *World Jounal of Microbiology and Biotechnology*, *15*, 321–327.

Jayasekara, R., Harding, I., Bowater, I., Christie, G. B. Y., & Lonergan, G. T. (2004). Preparation, surface modification and characterisation of solution cast starch PVA blended films. *Polymer Testing*, *23*, 17–27.

Mali, S. M., Grossmann, V. E., Garcia, M. A., Martino, M. N., & Zaritzky, N. E. (2002). Microstructural characterization of yam starch films. *Carbohydrate Polymers*, *50*, 379–386.

Mathew, S., & Abraham, T. E. (2008). Characterization of ferulic acid incorporated starch–chitosan blend films. *Food Hydrocolloids*, *22*, 826–835.

Park, H. R., Chough, S. H., Yun, Y. H., & Yoon, S. D. (2005). Properties of starch/PVA blend films containing citric acid as additive. *Journal of Polymers and the Environment*, *13*, 375–382.

Xiao, C. M., & Yang, M. L. (2006). Controlled preparation of physical cross-linked starch-g-PVA hydrogel. *Carbohydrate Polymers*, *64*, 37–40.

Xiong, H. G., Tang, S. W., Tang, H. W., & Zou, L. P. (2008). The structure and properties of a starch-based biodegradable film. *Carbohydrate Polymers*, *71*, 263–268.

Yang, H., Zhang, Q., Guo, M., Wang, C., Du, R. N., & Fu, Q. (2006). Study on the phase structures and toughening mechanism in PP/EPDM/SiO_2 ternary composites. *Polymer*, *47*, 2106–2115.

Yu, L., Dean, K., & Li, L. (2006). Polymer blends and composites from renewable resources. *Progress in Polymer Science*, *31*, 576–602.

Zhai, M. L., Yoshii, F., Kume, T., & Hashim, K. (2002). Syntheses of PVA/starch grafted hydrogels by irradiation. *Carbohydrate Polymers*, *50*, 295–303.

Zhai, M. L., Yoshii, F., & Kume, T. (2003). Radiation modification of starch-based plastic sheets. *Carbohydrate Polymers*, *52*, 311–317.

Zhang, X. H., Xu, W. J., Xia, X. N., Zhang, Z. H., & Yu, R. Q. (2006). Toughening of cycloaliphatic epoxy resin by nanosize silicon dioxide. *Materials Letters*, *60*, 3319–3323.

Zou, W. J., Peng, J., Yang, Y., Zhang, L. Q., Liao, B., & Xiao, F. R. (2007). Effect of nano-SiO_2 on the performance of poly (MMA/BA/MAA)/EP. *Materials Letters*, *65*, 725–729.